



US Army Corps
of Engineers
Waterways Experiment
Station

19960328 027

THE REMR BULLETIN

DTIC QUALITY INSPECTED 4

VOLUME 13, NUMBER 1

FEBRUARY 1996

NEWS FROM THE REPAIR, EVALUATION, MAINTENANCE, AND REHABILITATION RESEARCH PROGRAM

Uplift pressures resulting from flow along tapered rock joints

by Robert M. Ebeling and Michael E. Pace, U.S. Army Engineer Waterways Experiment Station

In 1992, investigators for the Electric Power Research Institute completed a study of 17 existing concrete gravity dams. The objective of this study was to identify key factors influencing uplift pressures. All dams were on instrumented rock foundations, and all had different foundation geology. An analysis of the uplift pressure measurements from each of these dams showed that foundation geology has a strong influence on uplift pressure distribution and that the geology controls the response of uplift pressure to changes in dam loading. The investigators discovered that an understanding of the flow within rock joints and the factors that affect the flow lead to a better understanding of the uplift measurements at the damsites, especially those rock formations possessing "tight" rock joints (Stone and Webster Engineering Corporation 1992).

One of the key stages in a stability evaluation of navigation and flood-control structures is the calculation (or assignment) of uplift pressures along a critical rock joint or joints within the foundation of the hydraulic structure. Using accurate piezometric instrumentation data at a site along with knowledge of the site geology is the preferred method for establishing uplift pressures. However, when instrumentation data are not available or when the reservoir levels to be analyzed exceed those for which the piezometric measurements were made, other procedures must be used to establish the distribution of flow and the

corresponding uplift pressures. Three procedures are widely used by engineers to establish the uplift pressures along an imaginary section or sections within the rock foundation. These are (1) a prescribed uplift distribution as given, for example, in an engineering manual specific to the particular hydraulic structure; (2) flow-net-computed uplift pressures; or (3) uplift pressures computed from flow within rock joints.

Under the REMR Research Program, a study was made that involved one-dimensional (1-D), steady-state laminar flow through a single permeable joint within a rock foundation. Its purpose was twofold: to introduce the fundamentals of flow within rock joints and to show how the dimensions of the joint (referred to as joint aperture) influence the computed uplift pressures. Specifically, the results of the study show the impact of a tapered aperture (i.e., constant change in taper with distance along a single rock joint) on the distributions of permeability and computed uplift pressures. The example model considered is that of a horizontal rock joint located below the base of a concrete dam monolith for the cases of low, medium, and high reservoir elevations.

Modeling Joint Flow: The Cubic Law

Laminar flow within a rock joint can be characterized in a simplistic form as flow between a pair of smooth parallel plates separated by a constant distance.

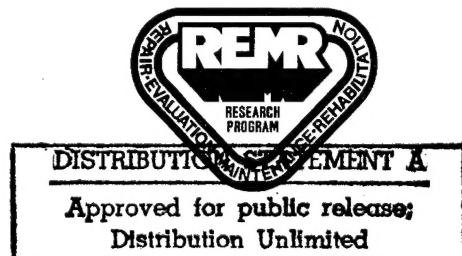
This distance is the joint opening or aperture, e (units of length). The flow rate per unit width is given by

$$Q = \frac{\gamma e^2}{12\mu} \cdot \left[-\frac{\partial h}{\partial l} \right] \cdot e \quad (1)$$

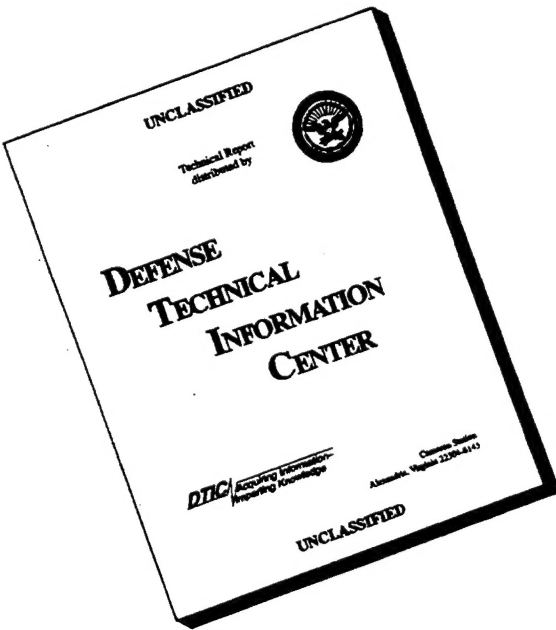
where γ is the unit weight of water (units of force per length cubed), e is the conducting aperture, and μ is the dynamic viscosity (e.g., slug/ft·sec (lb·sec/ft²)). The quantity of flow varies with the cube of the aperture e , hence the name "the cubic law." By analogy with Darcy's law, the equation for a single joint may be rewritten as

$$Q = K_{joint} \cdot [i] \cdot AREA_{flow} \quad (2)$$

where K_{joint} is the permeability, i is the hydraulic gradient, and $AREA_{flow}$ is the area of flow at any point along the single joint. Equation 2 can be used to compute the steady-state quantity of flow and distribution of uplift pressures given known values for γ and μ , the heads at each end of the joint, and the variation in aperture e with distance along the joint. Conventional 1-D steady-state seepage computer-program packages are available and can be used to



DISCLAIMER NOTICE



**THIS DOCUMENT IS BEST
QUALITY AVAILABLE. THE
COPY FURNISHED TO DTIC
CONTAINED A SIGNIFICANT
NUMBER OF PAGES WHICH DO
NOT REPRODUCE LEGIBLY.**

perform the seepage analysis for any distribution of e .

Tapered Joint

In the special case of a tapered joint, closed-form solutions can be developed for the quantity of flow within the joint and the distribution of uplift pressures along the length of the joint.

A tapered joint, such as the one shown in Figure 1, has linear variation in aperture with distance x along the joint (where x ranges in value from 0 to L). The equation for the conducting aperture e is given as

$$e(x) = \left[\frac{e_{out} - e_{in}}{L} \right] \cdot x + e_{in} \quad (3)$$

By Equation 1, the permeability at any point x varies in proportion to the square of the value of e .

The area of flow (per unit width) at any point along the joint is given as

$$K_{joint}(x) = \frac{\gamma}{12\mu} [e(x)]^2 \quad (4)$$

$$Area_{flow} = e(x) \quad (5)$$

By introducing Equations 3, 4, and 5 into Equation 1 with $Q_{in} = Q(x) = Q_{out}$ and for the known head boundary conditions on either side of the joint as shown in Figure 1, the following relationships are obtained after some mathematical manipulations are performed:

$$Q = 2 \left[\frac{\gamma}{12\mu} \right] e_{in}^2 (h_{in} - h_{out}) \frac{1}{L} \left[\frac{e_{out}^2 - e_{in}^2}{e_{out} + e_{in}} \right] \quad (6)$$

and

$$h(x) = h_{in} - \left\{ (h_{in} - h_{out}) \frac{1}{L} \left[\frac{e_{out}^2}{e_{out} + e_{in}} \right] \left[\frac{mx^2 + 2xe_{in}}{(mx + e_{in})^2} \right] \right\} \quad (7)$$

where

$$m = \frac{e_{out} - e_{in}}{L} \quad (8)$$

Equation 7 shows that the variation in head within a tapered joint is defined by five variables: the length of joint, the conducting apertures at the two ends of

the joint, the reservoir head, and the tailwater head. Note that Equation 7 does not explicitly include the term K_{joint} .

Example Problem: Raising the Pool Behind a Gravity Dam Founded on a Single Rock Joint

The case of a single horizontal rock joint located below the base of a

concrete monolith for the cases of low, medium, and high reservoir elevations is used to show the impact of joint aperture on uplift pressures. Figure 2 shows the hypothetical dam to be 300 ft high and 235 ft wide. It was assumed that jointing within the rock foundation was simplistic, i.e., a single rock joint parallel to and immediately below the dam-to-foundation interface. Changes in joint aperture during loading and/or unloading of the joint as a result of the construction of the dam and subsequent

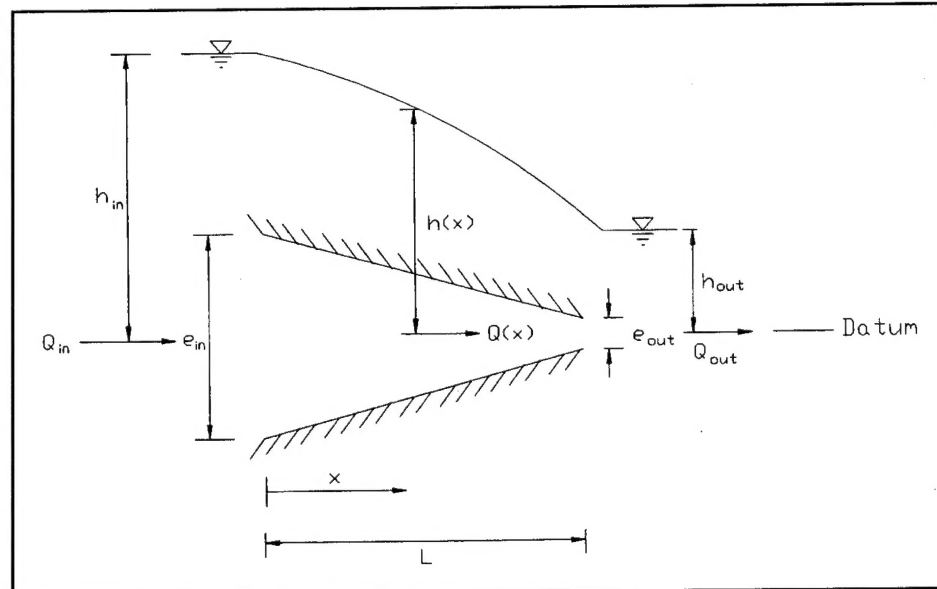


Figure 1. Variation of head along tapered joint as a function of position

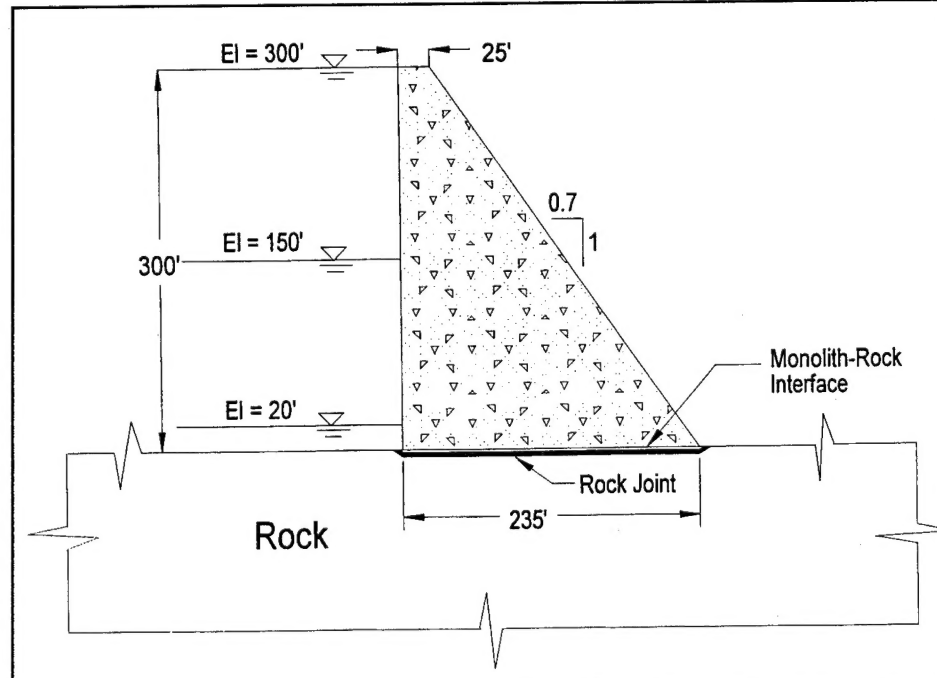


Figure 2. Geometry of dam used in study

filling of the reservoir are not included in these calculations.

Three different tapers for the rock joint in Figure 2 were investigated using Equation 7: no taper, uniform aperture ($e_{in} = e_{out}$); taper downstream ($e_{in} > e_{out}$); and taper upstream ($e_{in} < e_{out}$). By assigning the datum to be the center line of the horizontal rock joint (Figure 2), the uplift pressure at any point is equal to the head at the point times the unit weight of water (with elevation head equal to zero and the velocity head being negligible).

The variation in head (and thus, uplift pressure) along the 235-ft-long rock joint is shown in Figure 3 for the pool elevations equal to 20, 150, and 300 ft for $e_{in} = e_{out} = 4.92 \times 10^{-4}$ ft ($= 150 \mu\text{m}$ or 0.15 mm). This figure shows the uplift pressures to vary linearly along the joint for constant aperture.

Figure 4 shows the resulting variation in head with the joint tapered in the direction of flow (downstream) for the three pool elevations. In this example, e_{in} is set equal to $2e_{out}$, which results in the value of permeability at the toe (out) being one-fourth the magnitude of permeability at the heel (in).

Comparison of the distribution of head or, equivalently, uplift pressure in Figure 4 with that shown in Figure 3 indicates that for a given pool elevation, a taper downstream results in larger uplift pressures compared to the case of uniform aperture.

Figure 5 shows the resulting variation in head with the joint tapered in the direction opposite to flow (upstream) for the three pool elevations. In this example, e_{in} is set equal to $e_{out}/2$, which results in the value of permeability at the toe being four times the magnitude of permeability at the heel. Comparison of the distribution of head or, equivalently, uplift pressure in Figure 5 with those shown in Figure 3 indicates that for a given pool elevation, a taper upstream results in smaller uplift pressures compared to the case of uniform aperture.

When the taper of the joint downstream is increased from a factor of 2 (Figure 4) to a factor of 10 (Figure 6), larger uplift pressures result. Conversely, when the taper of the joint upstream is decreased from a factor of 1/2 (Figure 5) to a factor of 1/10 (Figure 7), smaller uplift pressures result. Lastly, the results in Figure 8

show that in the case of a tapered joint, the ratio of e_{in} to e_{out} dictates the distribution of uplift pressures. The magnitudes of e_{in} and e_{out} impact the quantity of flow (see Equation 6).

Conclusions

The principal results of this study of laminar flow along a single horizontal tapered rock joint are as follows:

- A uniform conducting aperture results in a linear variation in uplift pressures along the joint.
- A taper downstream results in larger uplift pressures compared to the case of uniform aperture.
- A taper upstream results in smaller uplift pressures compared to the case of uniform aperture.
- The larger or smaller the ratio of e_{in} to e_{out} is from a value of 1.0,

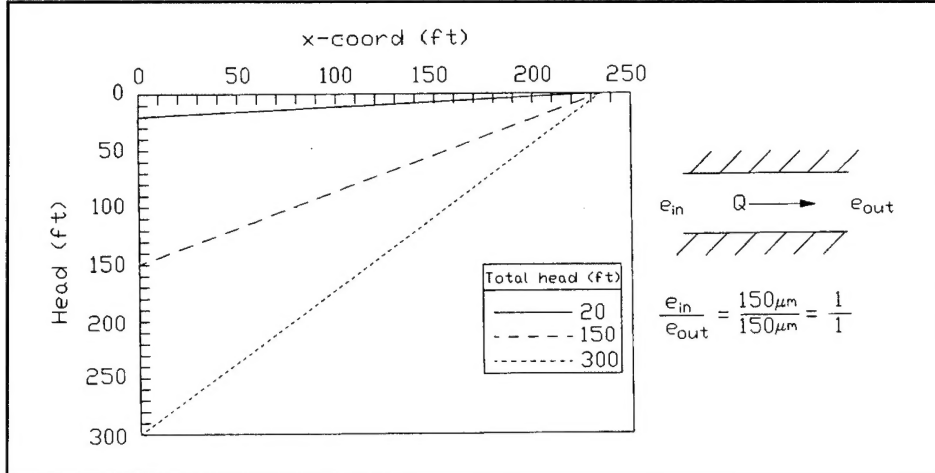


Figure 3. Variation in head along rock joint, $e_{in}/e_{out} = 1$

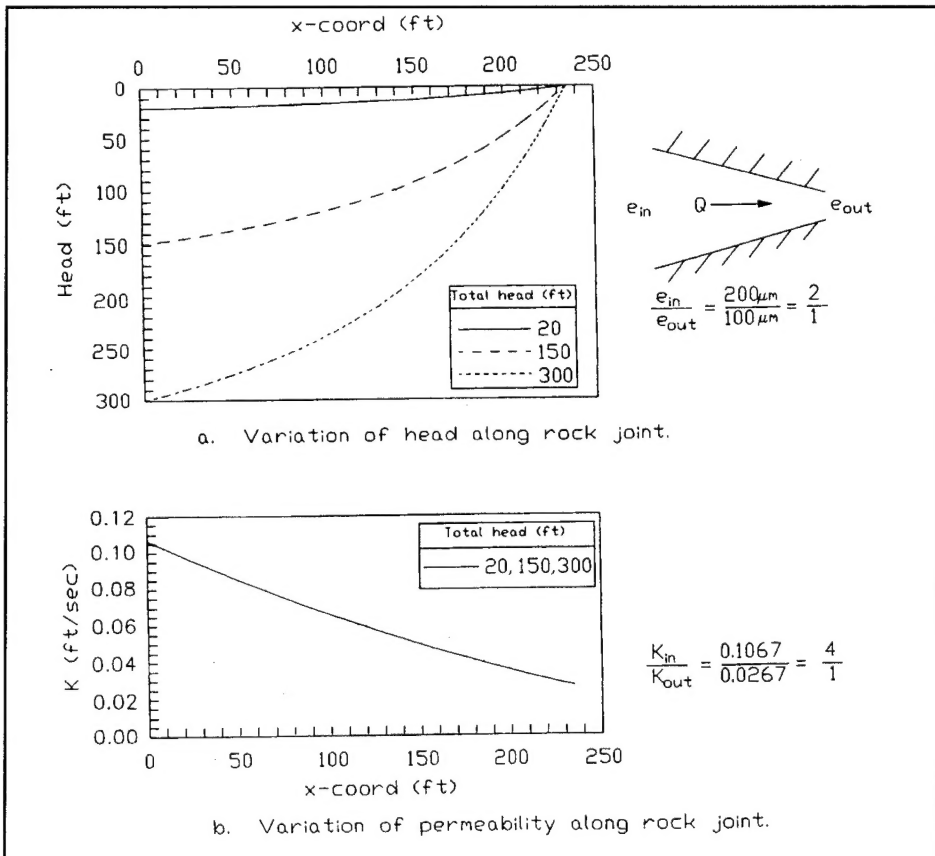


Figure 4. Head and permeability variation along rock joint, $e_{in}/e_{out} = 2/1$

the greater the departure of the uplift distribution is from a linear relationship along the joint.

- The magnitudes of e_{in} and e_{out} impact the quantity of flow.

For additional information, call Dr. Robert M. Ebeling at (601) 634-3458.

Reference

Stone and Webster Engineering

Corporation. (1992). "Uplift pressures, shear strengths, and tensile strengths for stability analysis of concrete gravity dams," report to Electric Power

Research Institute, EPRI TR-100345s, Vol 1.

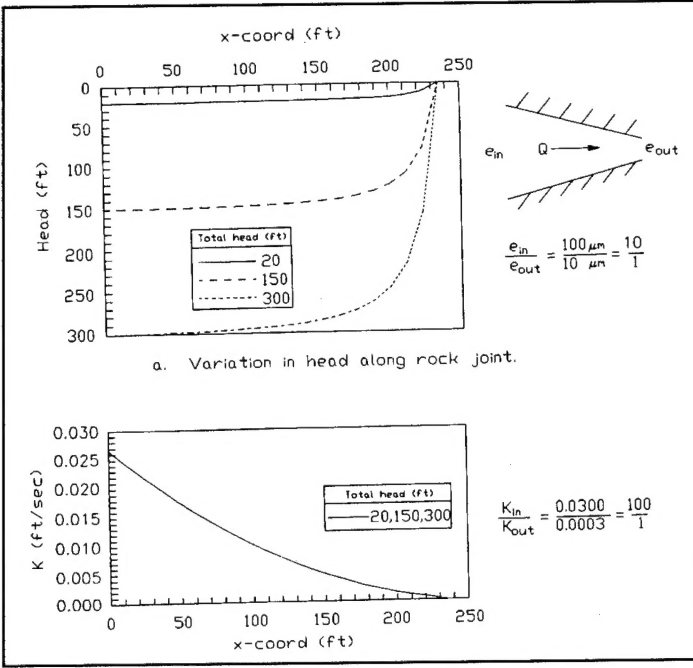
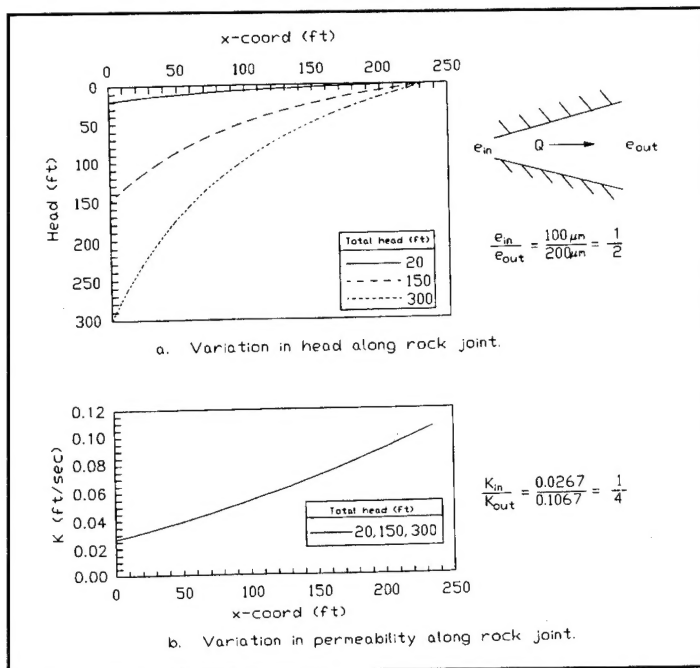


Figure 5. Head and permeability variation along rock joint, $e_{in}/e_{out} = 1/2$

Figure 6. Head and permeability variation along rock joint, $e_{in}/e_{out} = 10/1$

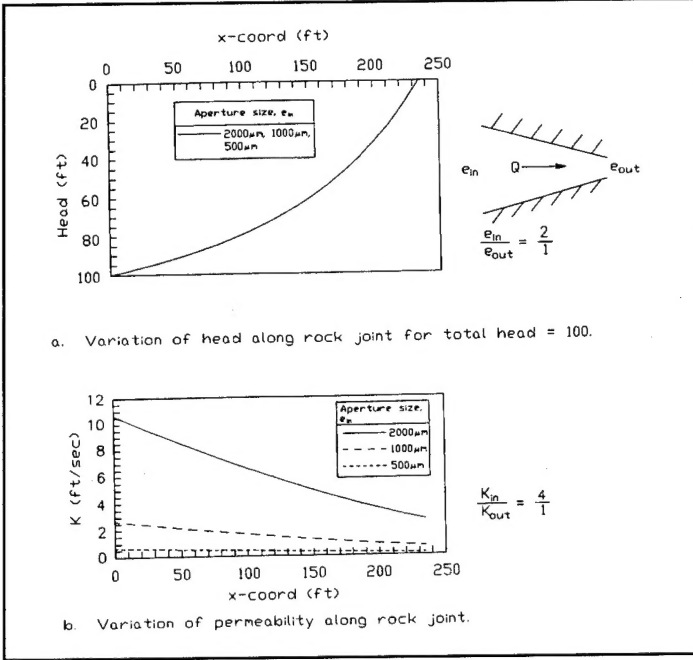
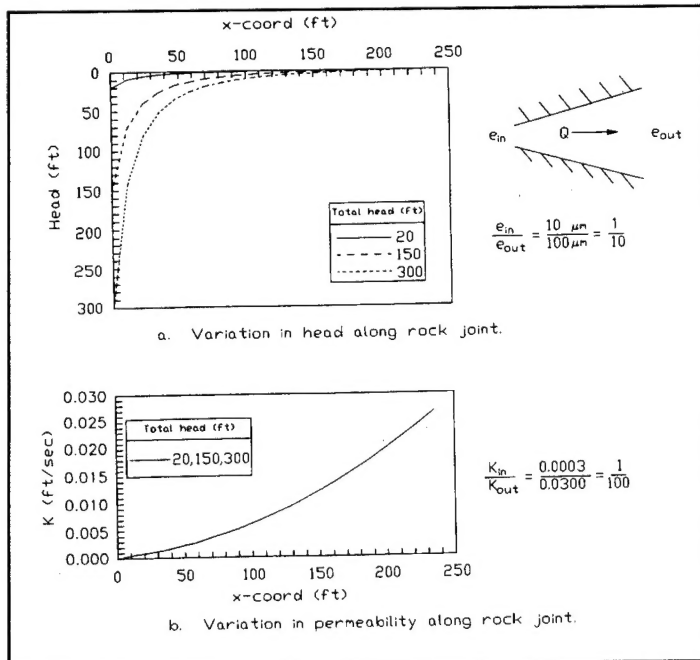


Figure 7. Head and permeability variation along rock joint, $e_{in}/e_{out} = 1/10$

Figure 8. Head and permeability variation along rock joint, $e_{in}/e_{out} = 2/1$

Variation in uplift pressures with changes in loadings along a single rock joint below a gravity dam

by Robert M. Ebeling and Michael E. Pace, U.S. Army Engineer Waterways Experiment Station

Navigation and flood-control structures are constantly being examined to determine whether they meet stability criteria. A common procedure for evaluating the safety of these structures is the conventional equilibrium method of analysis coupled with a prescribed uplift distribution as given, for example, in an engineering manual specific to that particular hydraulic structure. Many of these types of analyses are conducted without regard to how deformations impact the results. There are analytical tools such as the finite-element method (FEM) available that can consider the manner in which loads and resistance are developed as a function of the stiffness of the foundation rock (or soil), the structure, and the structure-to-foundation interface.

Under the REMR Research Program, a study was made of the impact of deformations on the resulting uplift distributions along a single joint located directly below a concrete dam monolith during and after construction and for subsequent initial filling of the reservoir.

Modeling Joint Flow: The Cubic Law

Flow within a rock joint can be characterized in a simplistic form as flow between a pair of smooth parallel plates separated by a constant distance. This distance is the joint opening or aperture, e . The flow rate per unit width is given by

$$Q = \frac{\gamma e^2}{12\mu} \left[-\frac{\partial h}{\partial l} \right] \cdot e \quad (1)$$

where γ is the unit weight of water, e is the conducting aperture, and μ is the dynamic viscosity. The quantity of flow varies with the cube of the aperture e , hence the name "the cubic law." By analogy with Darcy's law, the equation for a single joint may be rewritten as

$$Q = K_{joint} \cdot [i] \cdot AREA_{flow} \quad (2)$$

where K_{joint} is the permeability, i is the hydraulic gradient, and $AREA_{flow}$ (e times unit width) is the area of flow at any point along the single joint. Equation 2 can be used to compute the steady-state quantity of flow and distribution of uplift pressures (given known values for γ and μ), the heads at each end of the joint, and the variation in aperture e with distance along the joint. Conventional one-dimensional, steady-state seepage computer-program packages are available and can be used to perform the seepage analysis.

Modeling Joint Deformation

Laboratory studies have shown that joint aperture is not constant but varies with the stress applied normal to the joint. A mathematical relationship between the deformation of joints and the applied loading (or unloading) has been established based on laboratory tests on several different rocks and joint types. The deformation of a joint with applied normal stress is commonly referred to as joint closure/opening and is modeled for many types of joints and rocks as a hyperbolic function (as described in Bandis, Lumsden, and Barton (1983)). Figure 1 shows the hyperbolic relationship between joint

closure/opening with normal stress for initial loading and unloading of a single joint in moderately weathered sandstone using the model parameters given in Bandis, Lumsden, and Barton (1983). The size of the joint is described in terms of the mechanical aperture, E . Mechanical aperture E is distinguished from the conducting aperture e in that it is used in the cubic equation. The mechanical aperture of the joint is assumed to have an initial value of E_0 equal to 8.2×10^{-4} ft (250 μm or 0.25 mm) at zero stress normal to the joint, which is consistent with values typical of moderately weathered sandstone (Bandis, Lumsden, and Barton 1983) and is classified as a tight to partly open aperture according to Barton (1973). The changes in the mechanical aperture E with normal stresses shown in the upper portion of Figure 2 are computed as E_0 minus the joint closure of Figure 1.

An interrelationship between e and E in Barton, Bandis, and Bakhtiar (1985) was used to construct the relationship between conducting joint aperture e and normal stress shown in the lower portion of Figure 2 for a moderately weathered sandstone joint of typical joint roughness. The initial conducting joint aperture e at zero stress normal to the joint is equal to 2.75×10^{-4} ft (84 μm or 0.084 mm). Note that the

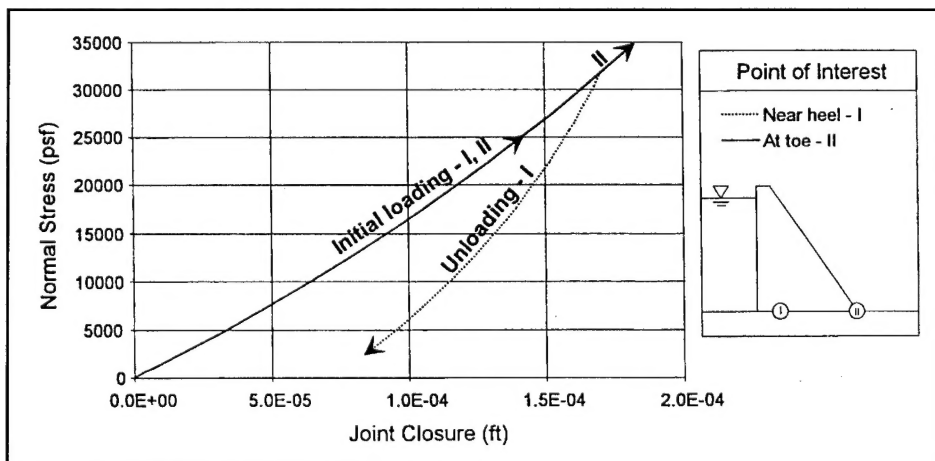


Figure 1. Joint closure and opening versus normal stress

conducting aperture e will always be less than the mechanical aperture E .

With the relationship between conducting aperture e and the normal stress shown in Figure 2, the relationship between permeability along a single joint and normal stress can be established by

$$K_{\text{joint}} = \frac{\gamma e^2}{12\mu} \quad (3)$$

Figure 3 shows the resulting relationship.

Modeling Joints Using the FEM of Analysis

The reactions of joints in rocks to changes in loadings can be modeled using a type of interface element developed by Goodman, Taylor, and Brekke (1968) to model the behavior of joints. This interface element is incorporated within the FEM program SOILSTRUCT (Ebeling, Peters, and Clough 1992). SOILSTRUCT is a general-purpose FEM program for two-dimensional (2-D) plane-strain analysis of soil-structure interaction

problems. SOILSTRUCT calculates displacements and stresses due to incremental construction and/or load application and can model nonlinear stress-strain material behavior. Two types of finite elements are used to represent the behavior of different materials comprising the monolith, its rock foundation, and the interface between them: a 2-D continuum element and an interface element.

Example Problem: Incremental Construction and First Flooding of a Gravity Dam Founded on Sandstone

The case of a concrete gravity dam constructed on weathered sandstone is used to show the impact of joint closure and opening on uplift pressures. Figure 4 shows the hypothetical dam to be 300 ft high and 235 ft wide. It was assumed that jointing within the sandstone foundation was simplistic, a single rock joint parallel to and immediately below the dam-to-foundation interface. Changes in joint aperture in this problem are a result of the construction of the dam and subsequent filling of the reservoir.

With the use of SOILSTRUCT, the model dam was constructed, and the pool was raised from the base to the crest of the dam in 19 incremental steps (13 for the dam and 6 for the reservoir). The dam and the sandstone foundation were assumed to be impervious, while all flow below the dam was assumed to be confined within the single sandstone joint. Twenty-nine interface elements were used to model the sandstone joint in the finite-element analysis, while 1,775 linear elastic, 2-D continuum elements were used to model the concrete dam and the foundation sandstone.

The constitutive model used for all 29 sandstone joint interface elements is illustrated in Figure 1. Figure 2 shows the resulting relationship between values for effective normal stresses and values for both mechanical and conducting apertures for the sandstone joint. Figure 3 demonstrates the resulting permeability of the rock joint based on the normal stresses. The variation of joint apertures (both E and e) due to changes in normal stresses resulting

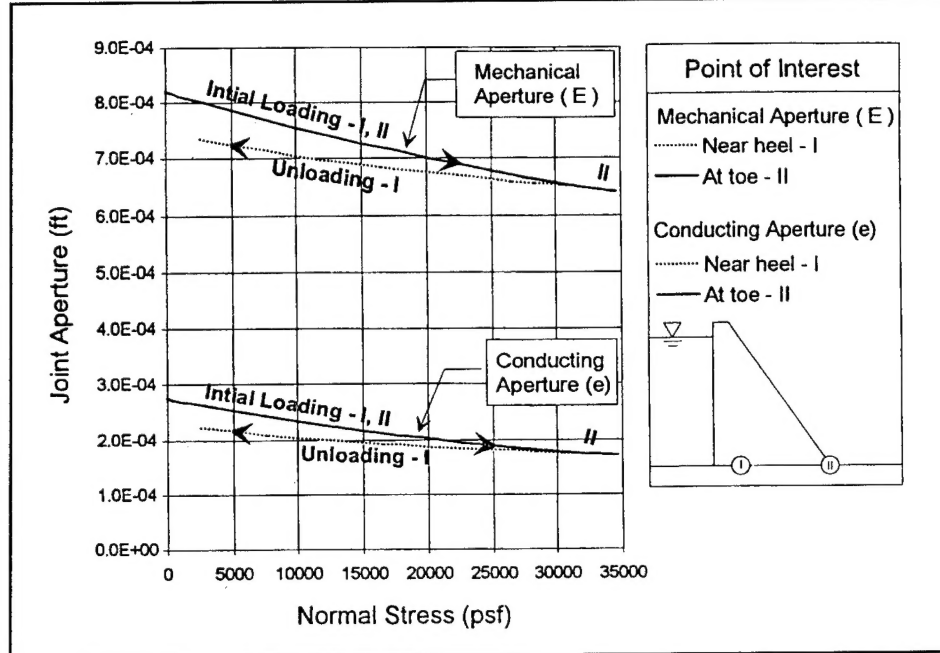


Figure 2. Joint aperture versus normal stress

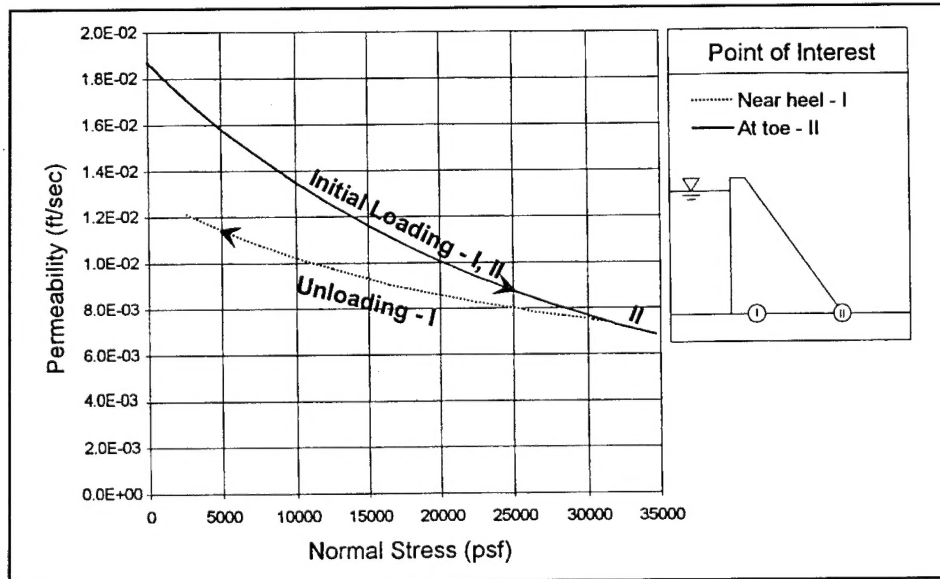


Figure 3. Permeability versus effective normal stress

from the construction of the dam and subsequent raising of the pool is shown in Figure 5. The initial joint aperture (prior to construction) was assumed to be uniform along the joint. The initial values for both the mechanical and conducting joint apertures ($E = 8.2 \times 10^{-4}$ ft and $e = 2.75 \times 10^{-4}$ ft) at two points along the joint are given in Figure 5. Loading or unloading of the sandstone joint is also identified in this figure at each end of the joint and for the four stages of loading reported in this figure.

Figure 6 shows the resulting distribution of uplift pressures along the single sandstone joint for pool elevations of 52, 170, and 300 ft. The results in this figure confirm that for the low and intermediate pool elevations, the distribution of uplift pressures along the sandstone joint is distinctly nonlinear from the heel to the toe. In fact, each of these two computed distributions is less than the linear distribution of uplift pressures which are typically assumed in equilibrium analyses. The distribution of nonlinear uplift pressures reflects the impact of changes of the distribution in conducting aperture with changes in loading/unloading along the sandstone joint.

Base separation was computed along nearly 50 ft of the base after the pool was raised to 300 ft. Full uplift pressure was assigned in this portion of the sandstone joint, as shown in Figure 6. Changes in joint aperture with this additional loading result in a change in uplift distribution as compared to the results from the intermediate and lower pool cases. Specifically, the distribution of uplift pressure is computed to be greater than that corresponding to a linear distribution of uplift pressure as shown in this figure.

Figure 7 displays the variation of uplift head computed at the heel, toe, and four points along the sandstone joint versus height of headwater. The nonlinear variation in uplift head with height of headwater at the four quarter-points along the joint reflects the changes in aperture with loading/unloading along the joint. It is interesting to note that a nonlinear variation in uplift with changes in pool elevations has been observed at several instrumented damsites, typically in foundations comprising tight joints. The joint size used in this analysis would be characterized as a tight sandstone joint.

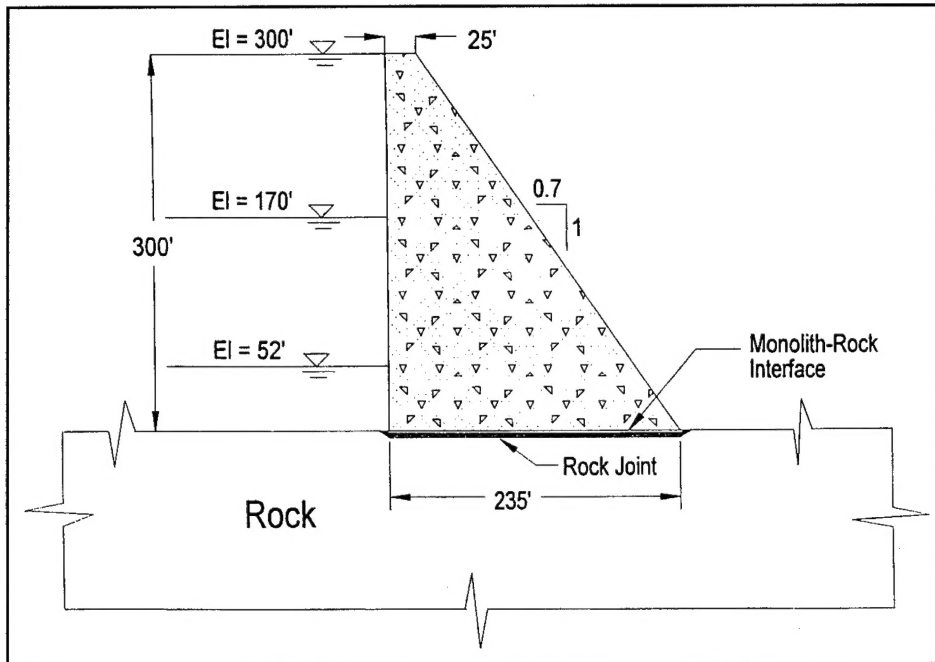


Figure 4. Geometry of dam used in study

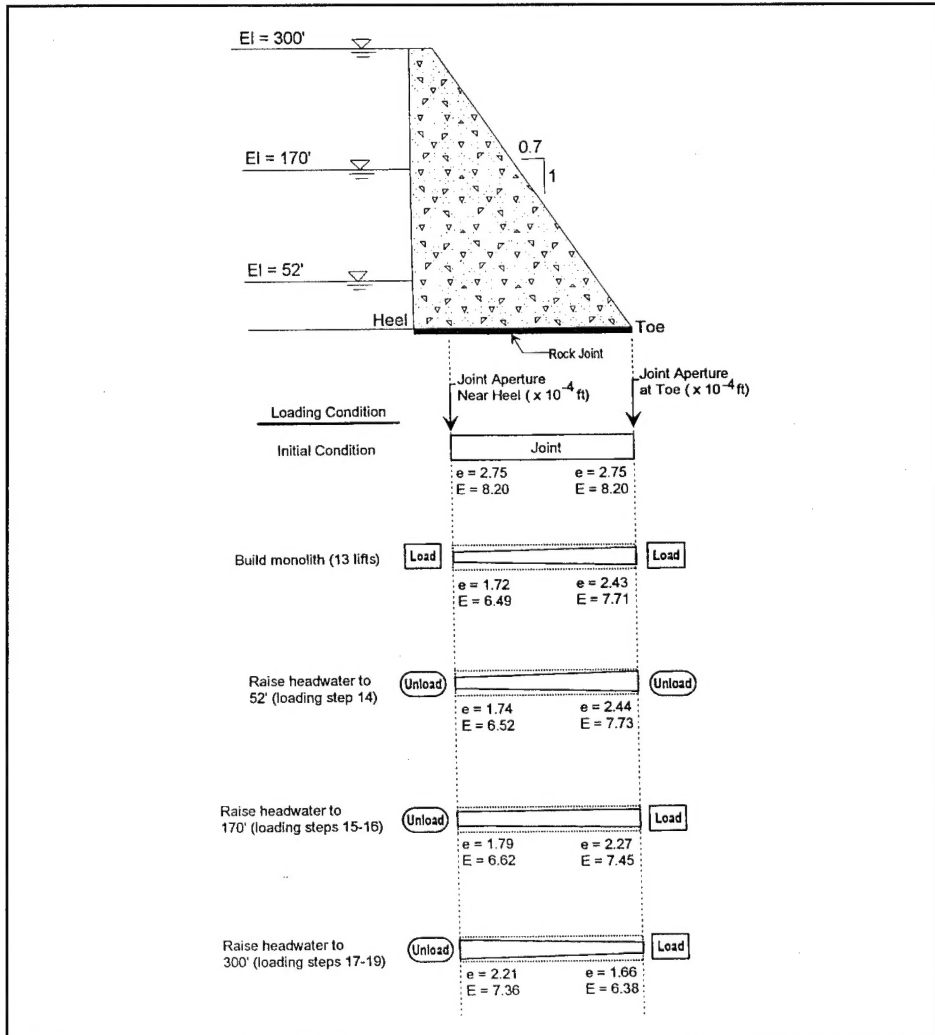


Figure 5. Effects of construction and water loading of monolith on joint aperture

The results of a finite-element analysis of an idealized dam founded on a sandstone foundation with a single tight joint illustrate the interrelationship between changes in joint aperture with loading/unloading of the joint. The changes in joint aperture result in changes in the distribution of uplift

pressures along the joint. This key aspect of the behavior of tight joints and corresponding uplift pressures as observed in this idealized problem is likely to be present in more complex, tight rock-joint foundations found at some damsites.

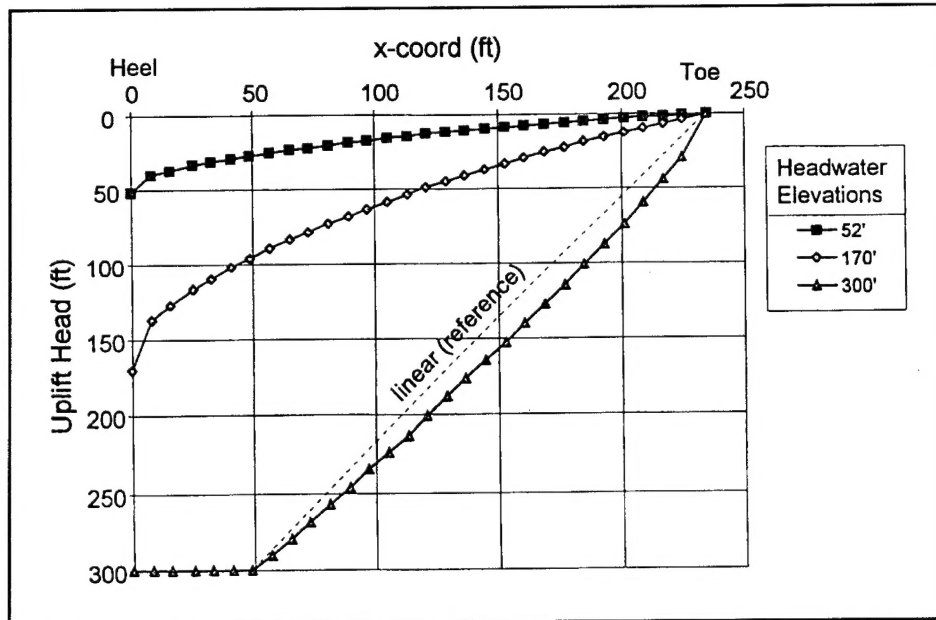


Figure 6. Variation in uplift head along a single joint with three headwater elevations

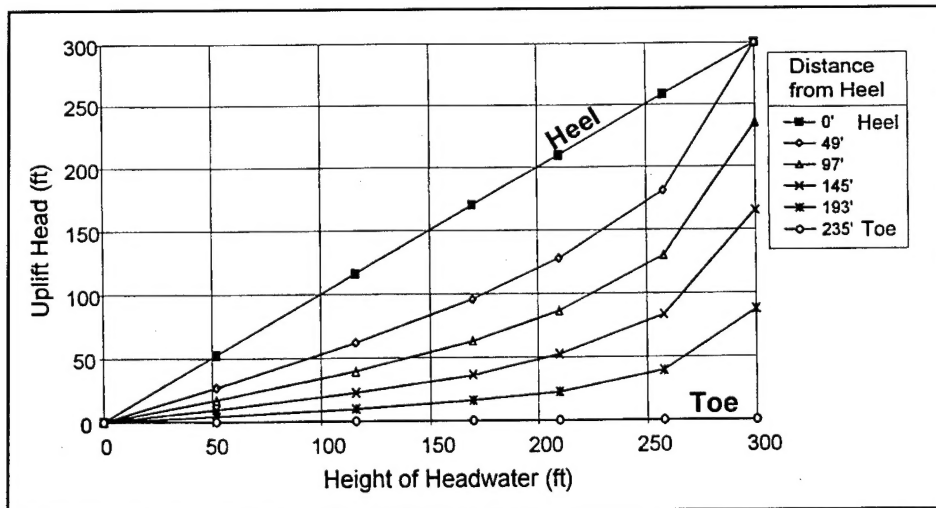


Figure 7. Variation of uplift head at six locations along the joint with headwater elevation

Conclusions

The principal results of this study are as follows:

- Joint aperture and permeability vary with normal stress.
- The distribution of uplift pressure along tight joints changes with the applied load and can be nonlinear.
- The change in piezometric head at any point along a tight rock joint can vary nonlinearly when compared with changes in reservoir head.

For additional information, call Dr. Robert M. Ebeling at (601) 634-3458.

References

- Barton, N.R. (1973). "Review of new shear strength criterion for rock joints," *Engineering Geology* 8, 287-332.
- Barton, N.R., Bandis, S.C., and Bakhtar, K. (1985). "Strength, deformation, and conductivity coupling of rock joints," *Int. J. Rock Mech. Min. Sci. & Geotech. Abstr.* 22(3), 121-140.
- Bandis, S.C., Lumsden, A.C., and Barton, N.R. (1983). "Experimental studies of scale effects on the shear behavior of rock joints," *Int. J. Rock Mech. Min. Sci. & Geotech. Abstr.* 20(6), 249-268.
- Ebeling, R.M., Peters, J.F., and Clough, G.W. (1992 May). "User's guide for the incremental construction soil-structure interaction program SOILSTRUCT," Technical Report ITL-90-6, U.S. Army Engineer Waterways Experiment Station, Vicksburg, MS.
- Goodman, R.E., Taylor, R.L., and Brekke, T.L. (1968). "A model for the mechanics of jointed rock," *Journal of the Soil Mechanics and Foundations Division*, No. SM3, American Society of Civil Engineers.

Stability of existing concrete structures

by Robert M. Ebeling, Ernest E. Morrison, and Reed L. Mosher, U.S. Army Engineer Waterways Experiment Station

A common procedure for determining whether older navigation and flood-control structures are meeting stability criteria is the conventional equilibrium method of analysis. Based largely on classical limit equilibrium analysis, this method does not consider deformation. Other analytical tools are available that can be used to consider the manner in which loads and resistance are developed as a function of the stiffness of the foundation rock (or soil), stiffness of the structure, and the structure-to-foundation interface. One of these is the finite-element method (FEM).

In a recent REMR research effort, two procedures formulated using the FEM were employed to evaluate the conventional equilibrium method. An existing earth-retaining structure was analyzed using these two FEM procedures and the conventional equilibrium method. The results of the three analyses were then compared.

Modeling Loss of Contact Along the Interface Using the FEM

Analytical procedures were developed that used the FEM analysis for problems concerned with loss of contact between the base of a gravity wall and its foundations. This situation occurs when structures are loaded so heavily that a gap develops in the interface region. Two approaches have been used to analyze this type of problem: one involving the modeling of a predetermined plane along which separation is presumed to develop using interface elements and the other involving the use of fracture mechanics concepts.

Base separation analysis using interface element

During Phase I of the REMR Research Program, the FEM program

SOILSTRUCT was expanded to model loss of contact between the gravity-wall base and the foundation using a procedure called the Alpha method (Ebeling, Duncan, and Clough 1990; Ebeling, Clough, Duncan, and Brandon 1992). SOILSTRUCT is a general-purpose FEM program for two-dimensional (2-D) plane-strain analysis of soil-structure interaction problems. It calculates displacements and stresses due to incremental construction and/or load applications and can model nonlinear stress-strain material behavior. Two types of finite elements are used to represent the behavior of different materials comprising the monolith, its rock foundation, and the interface between them: a 2-D continuum element and an interface element.

During each incremental following load analysis, each interface element along the base of the wall is checked to detect tensile stress at its center. If none is found, the following-load analysis proceeds as usual. When tensile stresses are observed in the interface elements, the incremental analysis is repeated using the Alpha method. Briefly, the principle of the procedure is to (1) factor the applied incremental load vector so that zero normal stress will result at the center of each of the interface elements which previously developed tensile stress at its center, (2) make the interface stiffness equal to zero, (3) convert the shear stress regime into an equivalent set of nodal point forces, (4) transfer this equivalent force into adjacent elements by applying it as an external force at the nodes, and (5) maintain equilibrium by subtracting the equivalent internal stress from within the interface element(s) used to formulate this force. The procedure is repeated until the total initial load increment has been applied.

Linear elastic fracture mechanics - discrete crack

A second FEM-based procedure for modeling crack development at the base of an earth-retaining structure in a following load analysis uses fracture mechanics concepts. Generally, linear elastic fracture mechanics (LEFM) relate the stress magnitude and distribution at the crack tip to the nominal stress applied to the structure; to the size, shape, and orientation of the crack or discontinuity; and to the material properties. The demand due to the loading(s) applied to the retaining structure, and specifically to the region of cracking, is represented by stress-intensity factors, K_I , K_{II} , and K_{III} for three cracking modes. Cracking Mode I is an opening mode, Mode II is a shearing mode, and Mode III is a tearing mode.

Conceptually, the stress-intensity factors indicate the rate at which the stress approaches infinity ahead of the crack tip for each of the three displacement modes. The stress-intensity factors characterize the magnitude of the crack-tip stress field for the potential cracking modes. The capacity of the material is characterized by the fracture toughness, K_c . Crack advance is monitored in an LEFM analysis by comparing the demand to capacity (e.g., K_I to K_{Ic}). The special-purpose FEM code MERLIN (Reich, Cervenka, and Saouma 1991) was used to perform the LEFM analysis for this study.

Description of the Lock Wall

Figure 1 shows a typical cross section for an existing lock wall. The wall is idealized as a 34.5-ft-long, 45-ft-wide (at the base) and 92-ft-tall massive concrete monolith retaining 83.7 ft of backfill with a water table 56 ft above the base.

Load Applied to the Lock Wall

In order to make a direct comparison between the conventional limit equilibrium method and the two finite-element methods, it was assumed that the wall was loaded by a predefined lateral pressure of given magnitude and distribution, as shown in Figure 1. Lateral pressures were established using conventional concepts for earth and water loadings on retaining-wall systems and were applied to the wall in a series of steps to determine the response of the structure to gradually increasing loads. Therefore, the magnitudes and distributions of the loadings were uncoupled from the action of the wall-foundation system. This form of loading is termed "following load analysis."

At-rest earth pressures were assigned normal to the plane extending vertically from the heel of the wall through the backfill (Figure 1). Lateral earth pressures corresponded to an at-rest earth-pressure coefficient K_0 of 0.45. A vertical shear force (also referred to as a downdrag force) was assigned to this plane. A shear force corresponding to a vertical earth-pressure coefficient K_v of 0.09 was assigned in all analyses.

The monolith and foundation were assumed to be impervious. Water flow from the backfill to the pool in front of the monolith was confined to the interface between the base of the monolith and the foundation. A linear head loss was assigned to this interface region where the monolith retained contact with the foundation. For the interface region where the monolith had separated from its foundation, hydrostatic water pressures corresponding to the hydrostatic head within the backfill were assigned. In the FEM analyses, water pressures were assigned along the interface, as shown in Figures 1 and 2.

Computed Results from Three Methods

Results of the following load analyses are summarized as follows:

- *Conventional equilibrium analysis (CEA).* Using the assumed linear compressive effective stress distribution directed normal to the base, the CEA resulted in a base

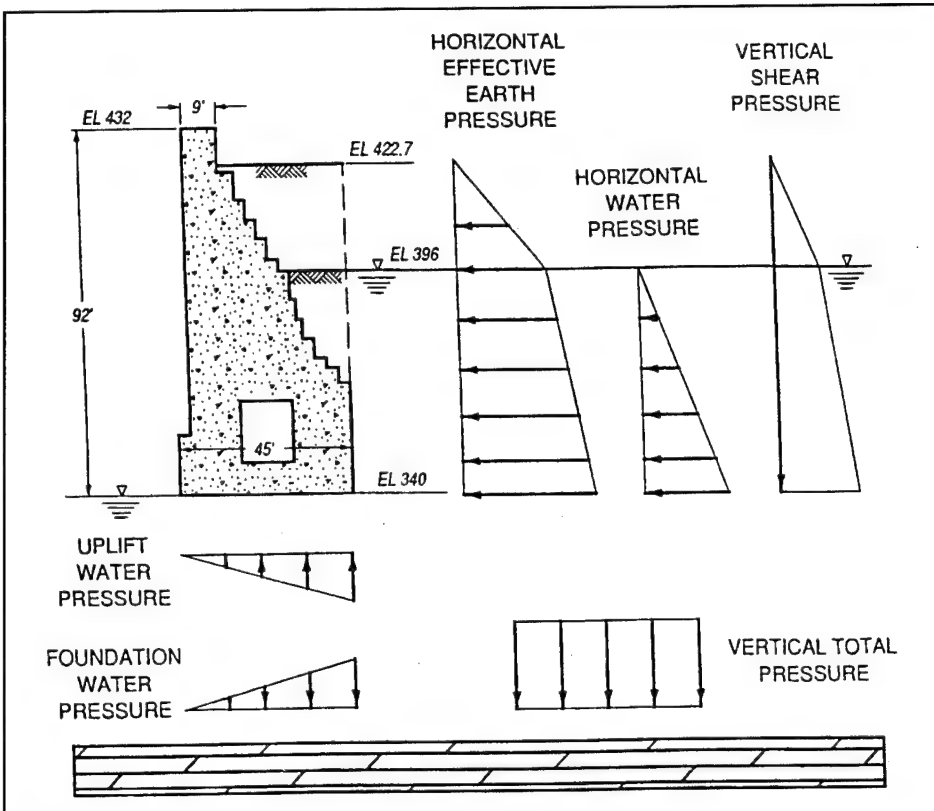


Figure 1. Cross section and following earth and water loadings

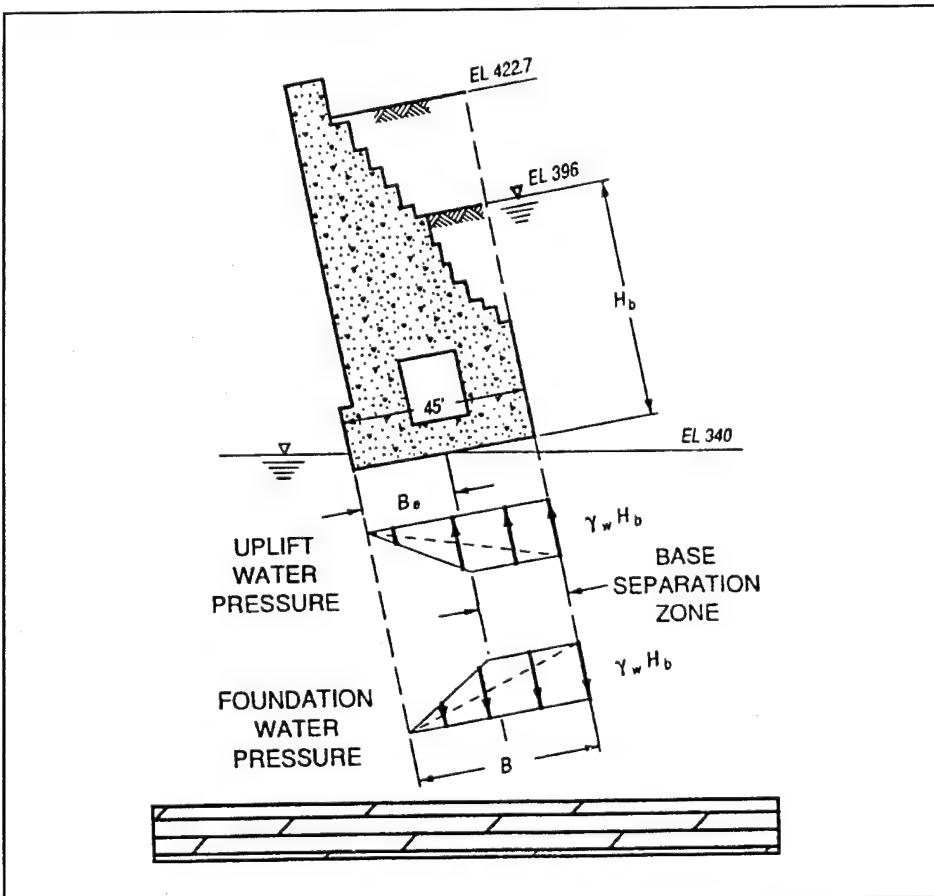


Figure 2. Water pressure distribution along the monolith-to-rock interface

area B_e in compression of 22.92 ft, or 50.9 percent of the base area in compression (B_e/B). This does not meet the design requirement of 75 percent for new structures of this type subjected to an extreme loading (i.e., a dewatered lock).

- **Base separation analysis using interface elements.** The value for B_e computed using the finite-element analysis (FEA) with interface elements was 32.65 ft, or 72.5 percent of the base area in compression. Figure 3 shows the normal effective stress distribution along the interface computed using both the FEA with interface elements and the equilibrium method of analysis. The resulting normal effective stress distribution from the FEA is distinctly nonlinear. The maximum normal effective pressure computed at the toe was 70,698 psf by the FEA method and 36,343 psf by the CEA method.

- **LEFM analysis.** An LEFM analysis of the wall was conducted using MERLIN (Headquarters, Department of the Army 1993) for the same lateral following earth and water loadings used in both the conventional equilibrium method of analysis and in the FEM analysis using SOILSTRUCT. The material toughness K_{lc} was set equal to zero along the interface between the monolith and the foundation. Uplift pressures were applied along the base as described previously. A series of six analyses, each with a different specified crack length, was performed using MERLIN to obtain an estimate of the crack length. The specified crack lengths for these analyses ranged from 6.0 to 13.5 ft in 1.5-ft increments. A crack length of 12.99 ft was estimated by interpolation of results of K_1 for the analysis with a crack length of 12 ft and the analysis with a crack length of 13.5 ft. Additional analyses were performed with refined meshes to determine a precise value for the final crack length. This procedure was repeated until the value of K_1 was less than 0.001 ksi [in.] $^{1/2}$. The final crack length computed using this approach was 13.02 ft, corresponding to B_e of 31.98 ft ($B_e/B = 71.1$ percent).

Figure 3 shows the normal effective stress distribution along the interface computed using both the FEA with interface elements and LEFM. Both analyses resulted in nonlinear normal effective stress distributions that were similar in shape. The maximum normal effective pressure was 70,698 psf by the FEA with interface elements and 105,603 psf by the LEFM.

Figure 4 shows the shear stress distribution along the interface computed using both the FEA with interface elements and LEFM. Both analyses resulted in nonlinear shear-stress distributions of similar shape.

Conclusions

The principal results of the three following-load analyses of the lock wall were as follows:

- The value of B_e/B computed using both FEM with interface elements (72.5 percent) was nearly equal to the value computed using LEFM (71.1 percent).
- The values of B_e/B computed using both FEM analyses were significantly greater than the 50.9 percent computed using CEA.
- Both FEM analyses resulted in nonlinear normal effective stress distributions, contrasting with the

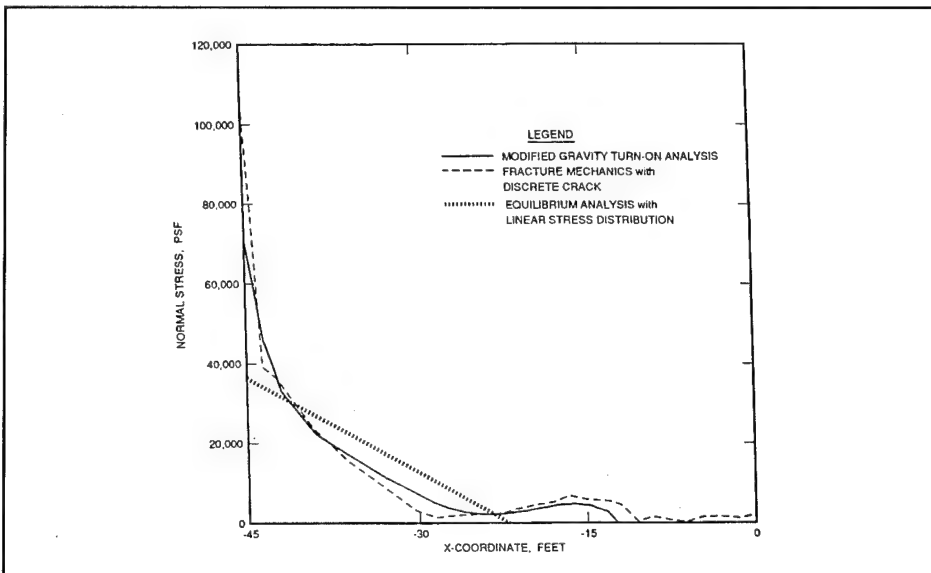


Figure 3. Normal stress distributions along the base of wall

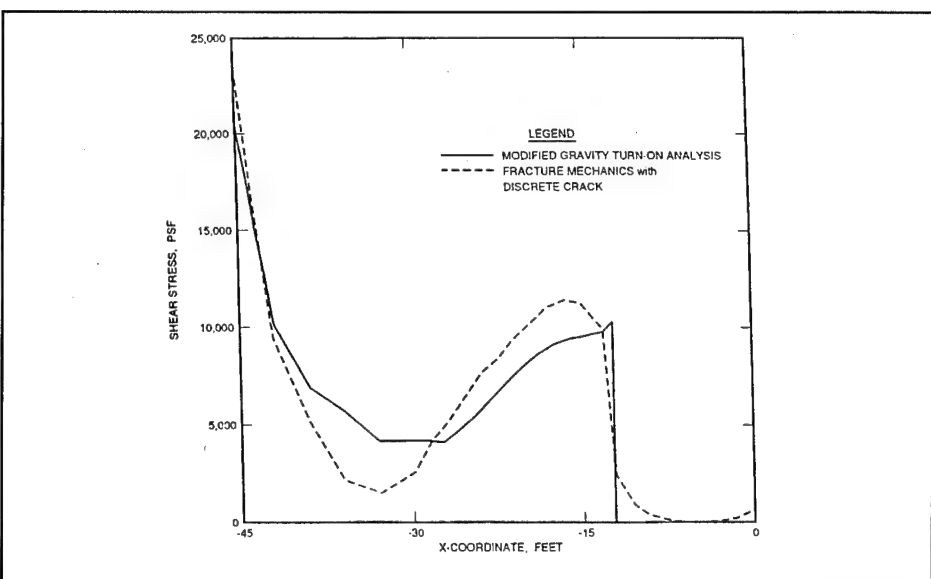


Figure 4. Shear stress distributions along the base of wall

assumed linear stress distribution used in the CEA.

For additional information, call Dr. Robert M. Ebeling at (601) 634-3458.

References

Ebeling, R.M., Clough, G.W., Duncan, J.M., and Brandon, T.L. (1992). "Methods of evaluating the stability

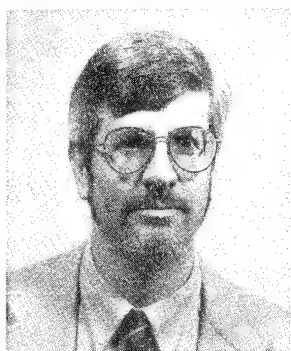
and safety of gravity earth retaining structures founded on rock," Technical Report REMR-CS-29, U.S. Army Engineer Waterways Experiment Station, Vicksburg, MS.

Ebeling, R.M., Duncan, J.M., and Clough, G.W. (1990). "Methods of evaluating the stability and safety of gravity earth-retaining structures founded on rock, phase 2 study," Technical Report ITL-90-7, U.S. Army Engineer

Waterways Experiment Station, Vicksburg, MS.

Headquarters, Department of the Army. (1993). "Fracture mechanics analysis of a gravity lock monolith," ETL 1110-2-344, Washington, D.C. Reich, R.W., Cervenka, J., and Saouma, V.E. (1991). "MERLIN user's manual," University of Colorado, Boulder, CO.

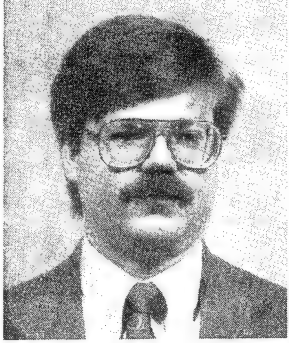
Dr. Robert M. Ebeling is a civil engineer at the U.S. Army Engineer Waterways Experiment Station (WES). His work has included a variety of geotechnical, structural, and earthquake engineering projects. He received a B.E.C.E. degree from Youngstown State University, Ohio; an M.E.C.E. from the University of California, Berkeley; and a Ph.D.C.E. from Virginia Tech. Dr. Ebeling is a Registered Professional Engineer in the State of California. He is a member of the American Society of Civil Engineers (ASCE) and the recipient of the ASCE State-of-the-Art in Civil Engineering Award. He is Principal Investigator for the REMR Work Unit 32640, "Stability and Remedial Measures for Existing Concrete Structures."



Dr. Reed L. Mosher is Chief of the Structural Mechanics Division, Structures Laboratory, WES. He has 18 years experience in the analysis and design of hydraulic structures such as locks, dams, and bridges. Dr. Mosher earned a B.S. degree in civil engineering from Worcester Polytechnic Institute, Worcester, MA; an M.S. degree in civil engineering from Mississippi State University at the Waterways Experiment Station Graduate Center; and a Ph.D. degree in civil engineering from Virginia Polytechnic Institute and State University, Blacksburg, VA.



Michael E. Pace is a civil engineer at WES. His work has included a variety of projects related to structural and geotechnical engineering. He received B.S.C.E. and M.C.E. degrees from Mississippi State University and has done postgraduate work in geotechnical engineering at Virginia Polytechnic Institute and State University. He is a member of the ASCE and the Society of American Military Engineers.



Ernest E. Morrison, Jr. is a research civil engineer working for the Information Technology Laboratory, WES. He received a B.S.C.E. degree from North Carolina State University and an M.S.C.E. degree from the University of Nevada at Reno. He is a Registered Professional Engineer in the State of Nevada.



Flow-net-computed uplift pressures along concrete monolith/rock foundation interface

by Robert M. Ebeling and Michael E. Pace, U.S. Army Engineer Waterways Experiment Station

One of the key stages in a stability evaluation of navigation and flood-control structures is the calculation (or assignment) of uplift pressures along the base of the hydraulic structure and/or along a critical rock joint or joints within the foundation. Using accurate piezometric instrumentation data at a site along with knowledge of the site geology is the preferred method for establishing uplift pressures. However, when instrumentation data are not available or when the reservoir levels to be analyzed exceed those for which the piezometric measurements were made, other procedures must be used to establish the distribution of flow and the corresponding uplift pressures.

Three procedures are widely used by engineers to establish the uplift pressures along an imaginary section or sections through the structure-foundation interface and/or along a section or sections within the rock foundation. These are (1) a prescribed uplift distribution as given, for example, in an engineering manual specific to the particular hydraulic structure; (2) uplift pressures computed from flow within rock joints; or (3) flow-net-computed uplift pressures. The latter method was selected for use in a recent REMR study involving two-dimensional (2-D), steady-state flow through a permeable rock foundation. The results of this study show the impact of homogeneous, anisotropic permeabilities (i.e., $K_x \neq K_y$) and the impact of base separation on the uplift pressures along the base of a rock-founded retaining monolith.

Steady-State Seepage Analysis

Today, analytical tools such as the finite-element method (FEM) are available to compute the distribution of heads and flow within permeable foundations. Most problems involve the analysis of steady-state seepage given problem-specific geometry and boundary conditions. An FEM model of two- or three-dimensional steady-state seepage

can consider homogeneous or heterogeneous regions comprising the flow regime as well as isotropic or anisotropic permeability within each of these regions. The Windows version of the Corps' FE seepage program (X8202 in the WES Library) (Tracy 1983), called FASTSEEP (Engineering Computer Graphics Laboratory 1993), was used in this analytical investigation of 2-D steady-state seepage.

Seepage Problem Analyzed

The case of a concrete gravity lock retaining wall founded on permeable rock was used in this study. Figure 1 shows the concrete monolith to be 82.7 ft high and 45 ft wide. This monolith has a base-to-height ratio of 0.54, which is within the range (0.33 to 0.7) that is typical for gravity earth-retaining monoliths (Ebeling et al. 1992). This particular monolith was

chosen for further study because its geometry (e.g., base-to-height ratio) is typical of gravity retaining monoliths and because this monolith has been extensively analyzed in the REMR Research Program for separation along the base of the monolith under extreme loading. The monolith was analyzed by means of (1) the conventional equilibrium method of analysis as well as the FEM with three different crack/crack propagation models; (2) a base separation analysis with the use of interface elements; (3) a base separation analysis with the smeared crack approach; and (4) a linear elastic fracture mechanics discrete crack analysis. In the case of the extreme loading (e.g., no lock pool) and a conservative assignment of material properties, all four analytical procedures showed that as much as 50 percent of the base of the monolith may separate from its rock foundation along their interface.

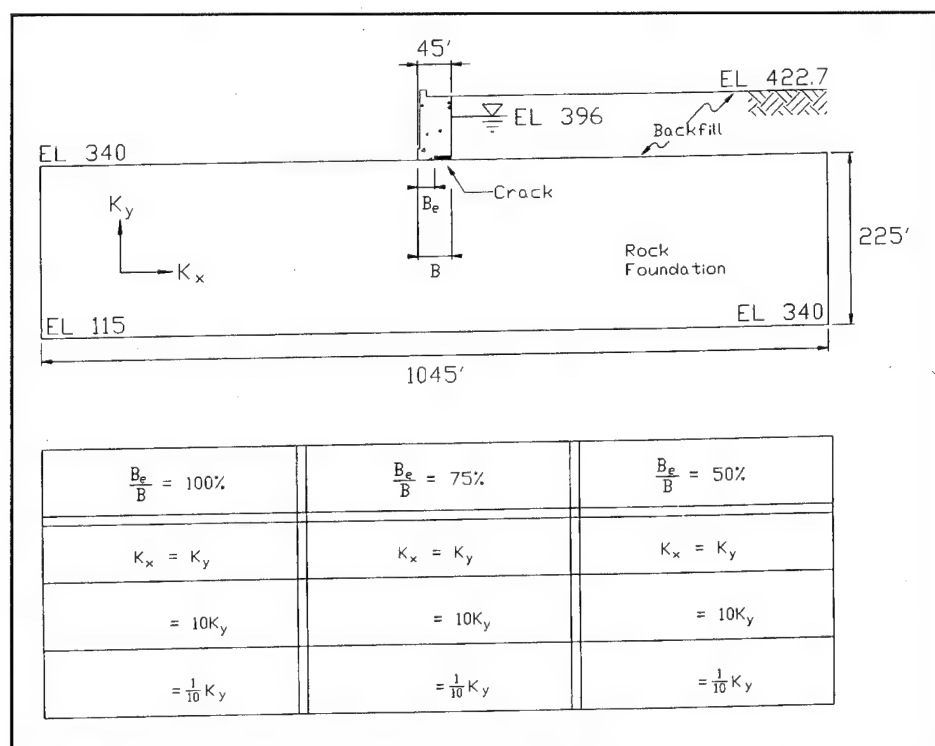


Figure 1. Problem geometry and cases considered

All nine seepage analyses assumed that the monolith was impermeable and that the permeable foundation was homogeneous. No drainage was included within the foundation in these problems. A typical set of dimensions is shown in Figure 1, along with a summary of the parameters that were varied in the nine seepage analyses. Three cases of monolith-to-foundation contacts were considered: full contact along the interface ($B_e/B = 100$ percent), an intermediate case of three-quarters contact along the interface ($B_e/B = 75$ percent), and the extreme case of only half of the monolith in contact with the foundation ($B_e/B = 50$ percent). For each case, three sets of foundation permeabilities ($K_x = K_y$, $K_x = 10K_y$, and $K_x = K_y/10$) were considered.

Flow Nets for Anisotropic Permeabilities with Full Contact Along the Interface

Figures 2 through 4 show the steady-state flow nets for the permeable foundation with $K_x = K_y$, $K_x = 10K_y$, and $K_x = K_y/10$, respectively, for a monolith in full contact with the rock foundation ($B_e/B = 100$ percent). The water table in the backfill is assumed to be at elevation (el) 396 ft, and the head in front of the monolith is assumed to be at el 340 ft.

A comparison of the flow net in Figure 3 for $K_x = 10K_y$ with that shown in Figure 2 for $K_x = K_y$ shows that along any given flow line below the monolith, there is less of a change in elevation between flow channels than that for the isotropic case (Figure 2). That is to say, the more permeable horizontal direction orients the flow channels in a more horizontal direction. The converse is true when the flow net in Figure 4 for $K_x = K_y/10$ is compared with that shown in Figure 2. In this case, the more permeable vertical direction orients the flow channels in a more vertical direction.

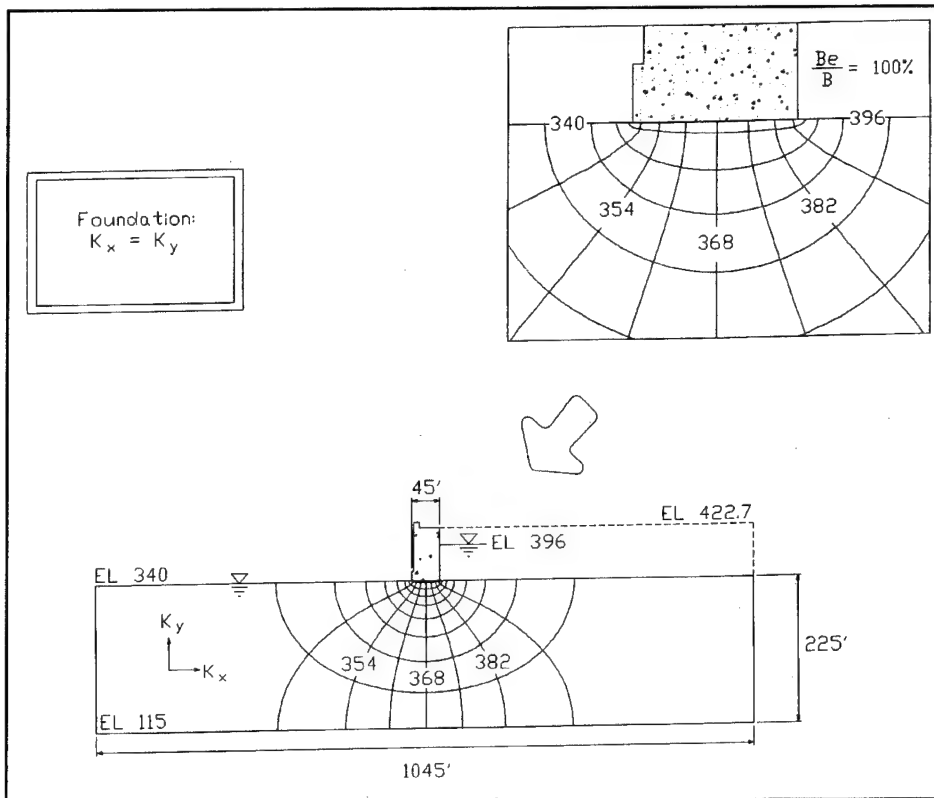


Figure 2. Results for $B_e/B = 100$ percent, $K_x \cdot b = y$

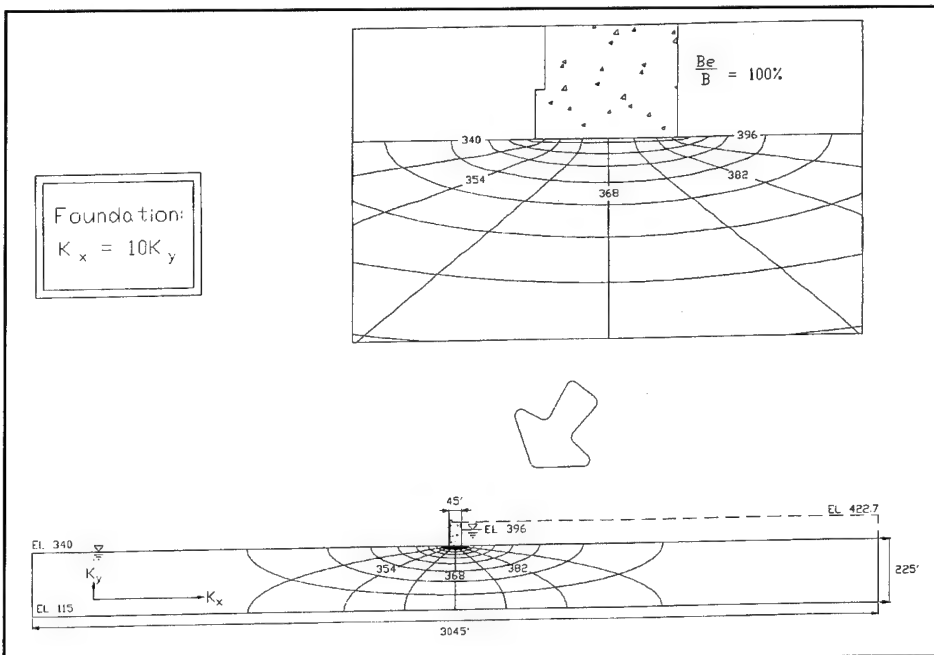


Figure 3. Results for $B_e/B = 100$ percent, $K_x = 10K_y$

Flow Nets for Isotropic Permeabilities with Partial Contact Along the Interface

Figures 2, 5, and 6 show the steady-state flow nets for the case of isotropic permeability ($K_x = K_y$) and 100, 75, and 50 percent, respectively, of monolith-to-rock base contact. In all analyses of monoliths with partial contact (i.e., a crack extending from the heel), full hydrostatic water pressures within the backfill (corresponding to a water table at el 396 ft) were assigned along the cracked portion of the interface. Comparison of the three figures shows that the symmetry of the flow channels is preserved about a vertical line located midway between the toe and the crack tip (which is the heel in Figure 2).

Uplift Pressures Along the Interface

The distributions of uplift pressures along the monolith-to-rock interface are shown in Figures 7, 8, and 9 for $B_e/B = 100$ percent (i.e., full contact), 75 percent, and 50 percent, respectively. Each figure shows the resulting uplift distribution for the cases of $K_x = K_y$, $K_x = 10K_y$, and $K_x = K_y/10$. The linear uplift distributions corresponding to flow confined along the interface (i.e., one-dimensional (1-D) flow) are also included in these figures. The three figures show four important results. First, 2-D seepage within the isotropic foundation alters the resulting distribution of uplift pressures when compared to uplift pressures resulting from 1-D flow. Second, the distributions of uplift pressures for the three ratios of permeabilities are nearly the same. Third, the distributions of uplift pressures from the 2-D analyses are antisymmetric to the distribution of uplift pressures for 1-D flow about a point midway between the tip of the crack and the toe of the wall. Finally, the point of antisymmetry is maintained midway between the crack tip and the toe for all crack lengths.

The resultant uplift force, equal to the area under each of the uplift pressure distributions, is the same value for each of the four analyses shown in

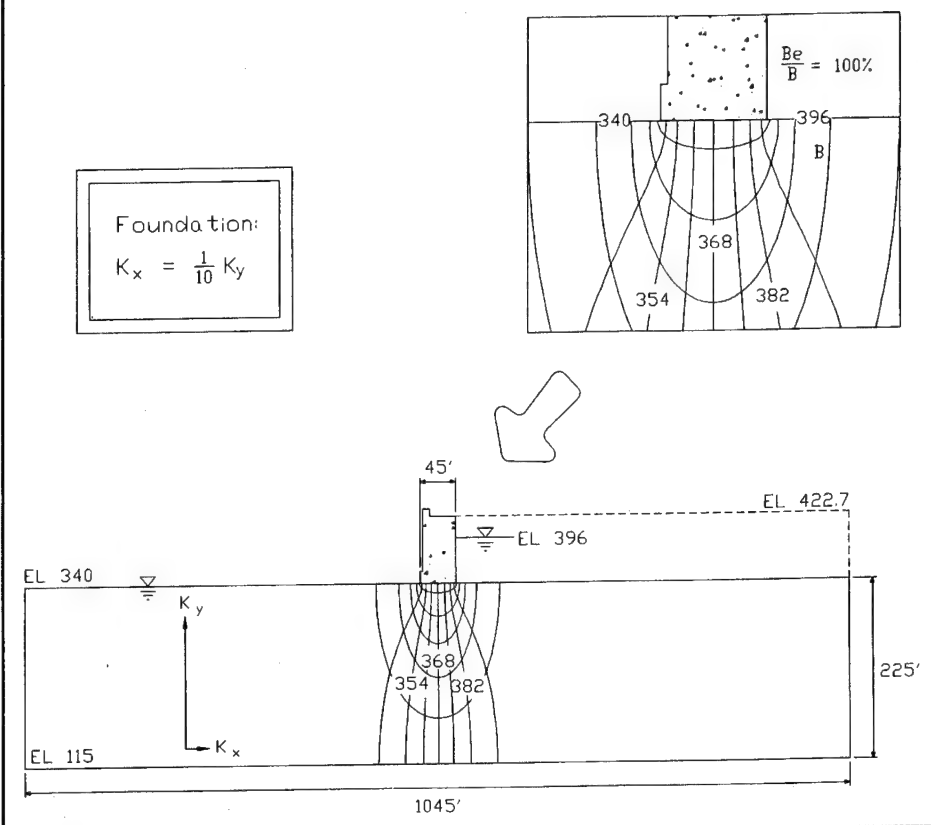


Figure 4. Results for $B_e/B = 100$ percent, $K_x = 1/10K_y$

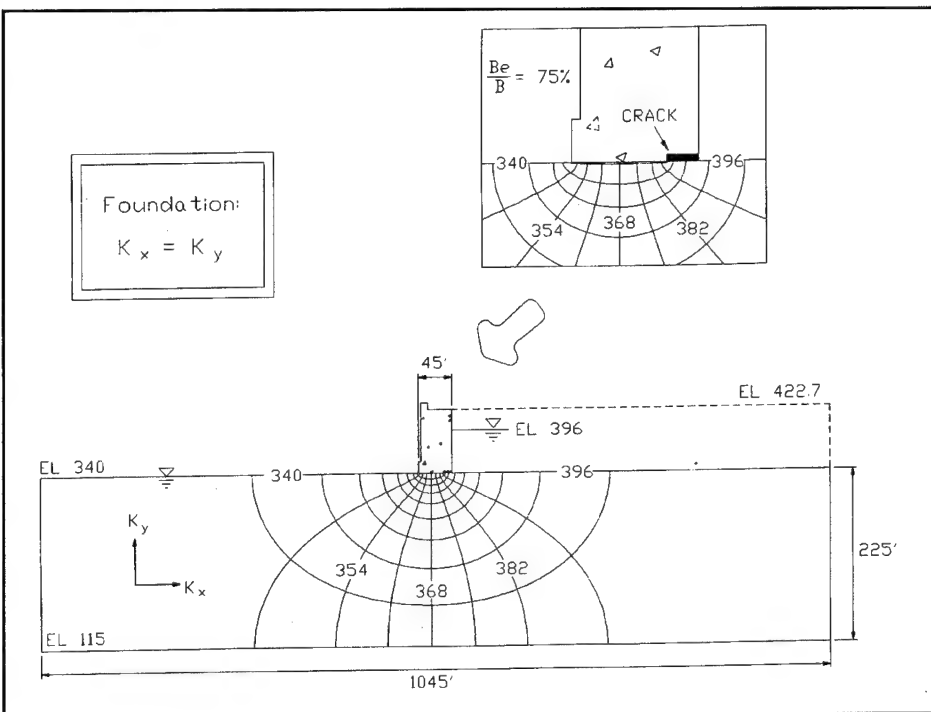


Figure 5. Results for $B_e/B = 75$ percent, $K_x = K_y$

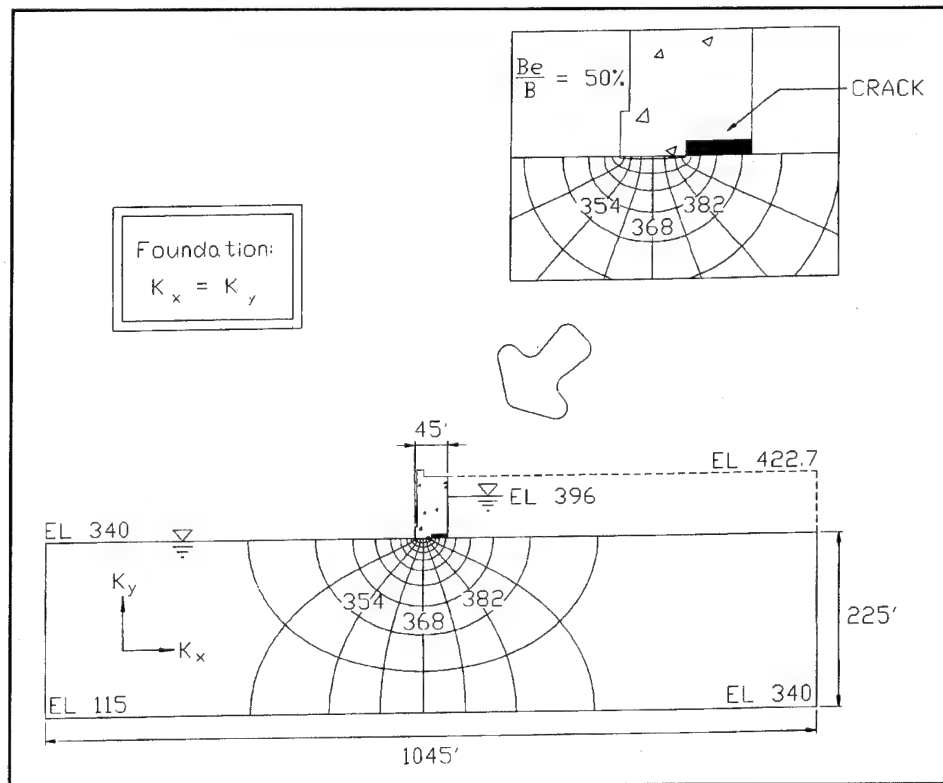


Figure 6. Results for $B_e/B = 50$ percent, $K_x = K_y$

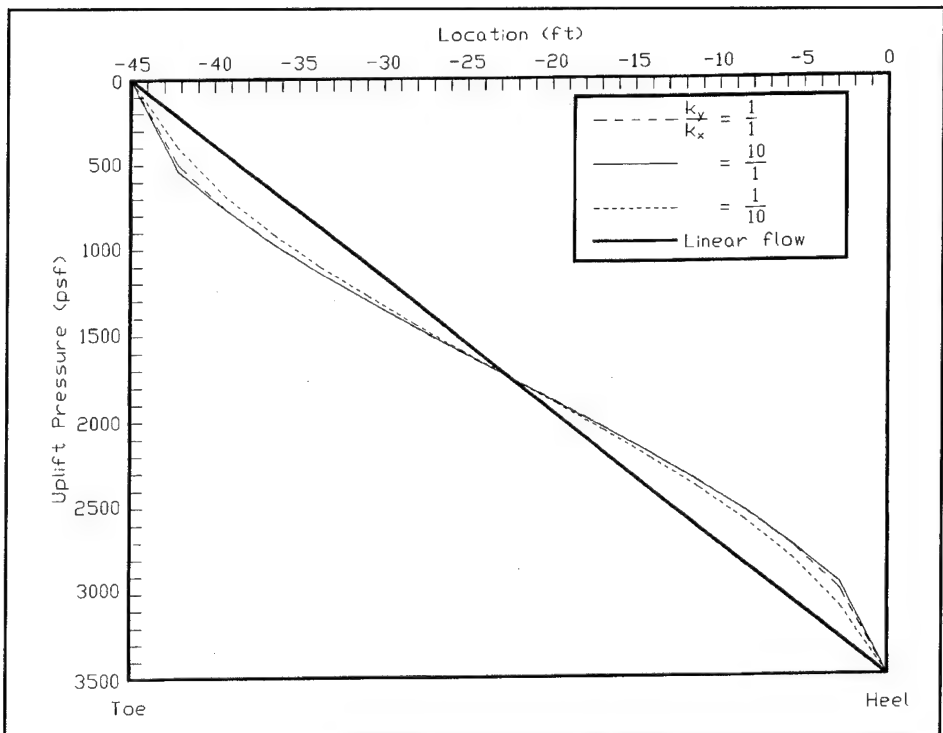


Figure 7. Uplift values for $B_e/B = 100$ percent

Figure 7. This is also the case for the results shown in Figures 8 and 9.

The resulting force for the linear uplift pressure distribution in Figure 7 (1-D flow) acts at a point along the interface that is two-thirds the distance from the toe to the heel, acting at a point 30 ft from the toe ($B_e = B = 45$ ft). The resultant uplift forces computed from the results of the other three 2-D analyses shown in Figure 7 act at points that are between 4 and 5 percent closer to the toe of the wall than the points for the linear uplift distribution. This difference is even less for the results shown in Figures 8 and 9.

Conclusions

The principal results of this study are as follows:

- Anisotropic permeabilities (i.e., $K_x \neq K_y$) orient the flow channel in the direction of larger permeabilities. This effect is observed in the resulting 2-D steady-state seepage flow net.
- Given a prescribed crack length, the magnitude of the resulting uplift force is equivalent for the 1-D analysis to the uplift forces computed from the three 2-D analyses ($K_x = K_y$, $K_x = 10K_y$, and $K_x = K_y/10$).
- The distributions of uplift pressure along the monolith-to-rock interface calculated using 2-D FE seepage analyses are similar but not exactly equivalent to the distribution from 1-D seepage analyses. Even though the resultant uplift forces are equal in magnitude, differences in the distributions of uplift pressures between the two analyses result in the uplift forces acting at different points along the interface.

The authors caution against making generalities based on the results of this study to more complicated seepage problems. They attribute many of the similarities in the previously stated 1- and 2-D study results to the following features of the nine idealized problems:

- The distance from the toe of the monolith to the left extent of the finite-element mesh (i.e., a location of a flow or head boundary condition) was large and equal to the distance from the heel to the right extent of the mesh (another flow or head boundary condition).

- The base of the monolith was parallel to the primary flow channels in all four seepage analyses.
- The permeable foundation was modeled as homogeneous.
- The primary flow channel immediately below the monolith was nearly horizontal as was the rock-to-monolith interface.
- No drainage features were included in the foundation.

Any one of these factors will impact the conclusions stated previously and will contribute to larger differences in the results between the different types of seepage analyses when compared to the results of this study.

For additional information, call Dr. Robert M. Ebeling (601) 634-3458.

References

- Ebeling, R.M., Clough, G.W., Duncan, J.M., and Brandon, T.L. (1992). "Methods of evaluating the stability and safety of gravity earth retaining structures founded on rock," Technical Report REMR-CS-29, U.S. Army Engineer Waterways Experiment Station, Vicksburg, MS.
- Engineering Computer Graphics Laboratory. (1993). "FASTSEEP." Brigham Young University, Provo, UT.
- Tracy, F.T. (1983). "User's guide for a plane and axisymmetric finite element program for steady-state seepage problems," Instruction Report K-83-4, U.S. Army Engineer Waterways Experiment Station, Vicksburg, MS.

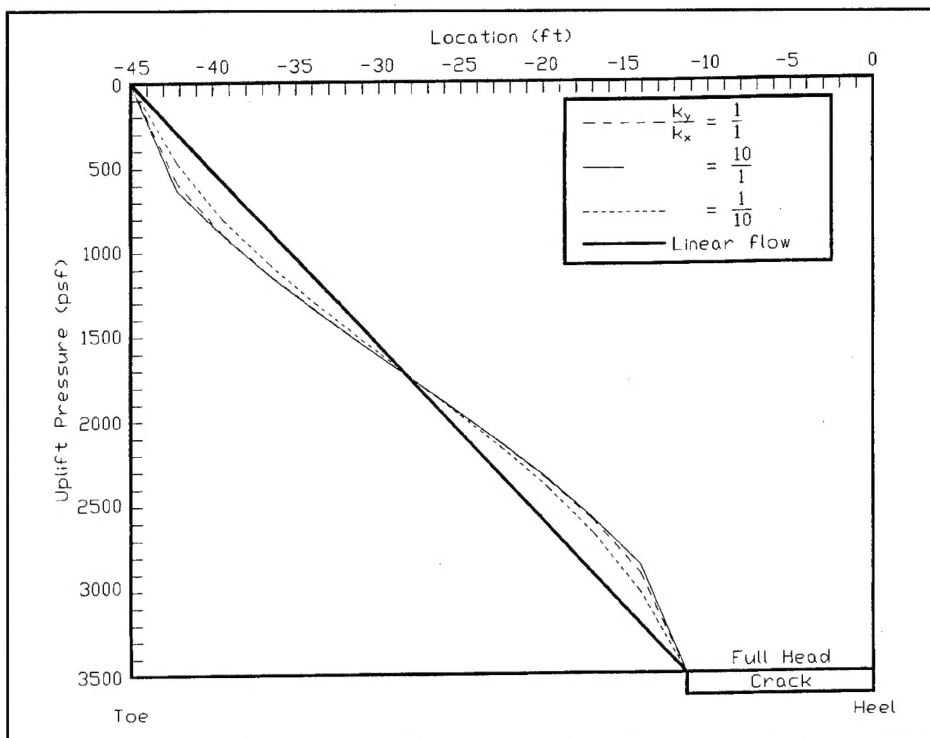


Figure 8. Uplift values for $B_e/B = 75$ percent

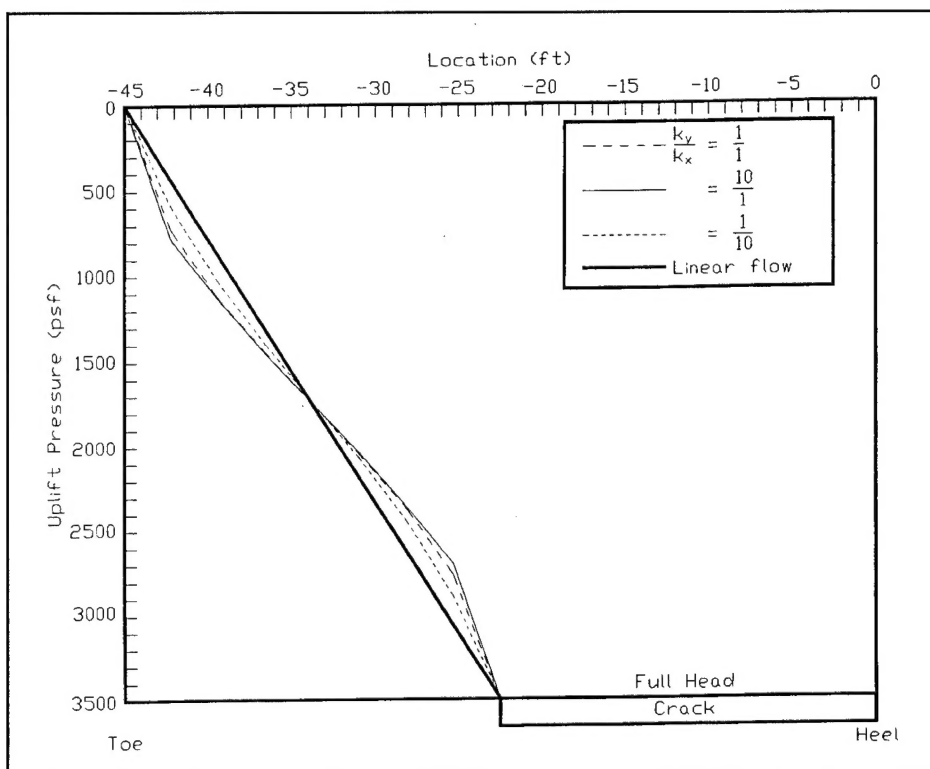


Figure 9. Uplift values for $B_e/B = 50$ percent

Call for Papers

The American Society of Civil Engineers (ASCE) Facilities Management Committee's *Infrastructure Condition Assessment Conference* will be held in Boston, MA, in August 1997. Managing our civil infrastructure has become a national priority, and condition assessment is at the core of infrastructure decision making. This timely subject covers many areas including buildings, pavements, railroads, bridges, utilities, air and water quality, ports, inland navigation, and others.

The objective of this conference is to provide a forum for the exchange of condition assessment experiences and practices of people from all engineering disciplines including academics, researchers, practitioners, planners, and students of infrastructure science and technology. The emphasis will be on the use and potential use of technologies and systems for assessing and predicting

the condition of our civil infrastructure. Papers from both research and practice-oriented topics are encouraged. Some of the topics proposed for this conference are as follows:

- Deterioration modeling
- Data collection
- Data analysis
- Nondestructive testing
- Instrumentation
- Multimedia
- Visualization
- Virtual reality
- Standards and policies
- Rating systems and interpretation
- Inspection, methods, and technology

Interested authors are invited to submit three copies of an abstract, no more than 250 words in length. The abstracts should be received at the following address no later than August 1, 1996, and must include full title and

give the affiliation and mailing address of the author(s).

Dr. Samer Madanat, Program Chair
School of Civil Engineering
Purdue University
West Lafayette, Indiana
47907-1284
Phone: (317) 494-3954
Fax: (317) 496-1105
madanat@ecn.purdue.edu

Abstracts will be reviewed and authors will be notified on or before January 3, 1997. Final acceptance will be based on the camera-ready copy of the final manuscript due by April 18, 1997.

In accordance with ASCE policy, authors cannot be reimbursed by ASCE for expenses incurred in preparation of abstracts. Authors who submit final papers imply a firm agreement to present their paper and to register and attend the Conference.

PROSPECT Course on REMR Condition Index Inspections and Management Systems Being Offered

The Proponent Sponsored Engineer Corps Training (PROSPECT) Program is offering a course on REMR Condition Index Inspections and Management Systems for selected Civil Works structures. The course will cover navigation lock miter gates and concrete lockwall monoliths, as well as steel sheet-pile structures such as retaining walls and mooring cells.

This 36-hr course includes both classroom instruction and field exercises,

where actual inspection techniques are performed. The class closes with instruction on the use of custom software programs for managing and analyzing the inspection and condition index databases.

A minimum class size of 20 students is required. REMR Field Review Group members are strongly encouraged to promote this course within their Divisions. If this class succeeds, additional courses on a variety of

structure types will be offered regularly in the future.

The course is scheduled for August 1997 at Old Hickory Lock in the Nashville District. The point of contact is Mr. Dave McKay, CECER-FL-P, Construction Engineering Research Laboratories, P.O. Box 9005, Champaign, IL 61826-9005; telephone (217) 398-5487; fax (217) 398-5220; or e-mail d-mckay@cecer.army.mil.



Featured In This Issue

| | |
|----------------------------------------------------------------------------------------------------------------|----|
| Uplift pressures resulting from flow along tapered rock joints | 1 |
| Variation in uplift pressures with changes in loadings along a single rock joint below a gravity dam | 5 |
| Stability of existing concrete structures | 9 |
| Flow-net-computed uplift pressures along concrete monolith/rock foundation interface | 13 |
| Call for Papers | 18 |
| PROSPECT Course on REMR Condition Index Inspections and Management Systems Being Offered | 19 |



PRINTED ON RECYCLED PAPER



The REMR Bulletin is published in accordance with AR 25-30 as one of the information exchange functions of the Corps of Engineers. It is primarily intended to be a forum whereby information on repair, evaluation, maintenance, and rehabilitation work done or managed by Corps field offices can be rapidly and widely disseminated to other Corps offices, other U.S. Government agencies, and the engineering community in general. Contribution of articles, news, reviews, notices, and other pertinent types of information are solicited from all sources and will be considered for publication so long as they are relevant to REMR activities. Special consideration will be given to reports of Corps field experience in repair and maintenance of civil works projects. In considering the application of technology described herein, the reader should note that the purpose of *The REMR Bulletin* is information exchange and not the promulgation of Corps policy; thus guidance on recommended practice in any given area should be sought through appropriate channels or in other documents. The contents of this bulletin are not to be used for advertising, or promotional purposes, nor are they to be published without proper credits. Any copyright material released to and used in *The REMR Bulletin* retains its copyright protection, and cannot be reproduced without permission of copyright holder. Citation of trade names does not constitute an official endorsement or approval of the use of such commercial products. *The REMR Bulletin* will be issued on an irregular basis as dictated by the quantity and importance of information available for dissemination. Communications are welcomed and should be made by writing U.S. Army Engineer Waterways Experiment Station, ATTN: Lee Byrne (CEWES-SC-A), 3909 Halls Ferry Road, Vicksburg, MS 39180-6199, or calling (601) 634-2587.

ROBERT W. WHALIN, PhD, PE
Director

CEWES-SC-A
OFFICIAL BUSINESS

BULK RATE
U.S. POSTAGE PAID
Vicksburg, MS
Permit No. 85

DEPARTMENT OF THE ARMY
WATERWAYS EXPERIMENT STATION, CORPS OF ENGINEERS
3909 HALLS FERRY ROAD
VICKSBURG, MISSISSIPPI 39180-6199